Cell, Vol. 122, 901–913, September 23, 2005, Copyright ©2005 by Elsevier Inc. DOI 10.1016/j.cell.2005.06.041

Mechanistic Link between PKR Dimerization, Autophosphorylation, and eIF2α Substrate Recognition

Madhusudan Dey,[1] Chune Cao,[1] Arvin C. Dar,[3,4] Tomohiko Tamura,[2] Keiko Ozato,[2] Frank Sicheri,[3,4] and Thomas E. Dever[1,*]

[1]Laboratory of Gene Regulation and Development
[2]Laboratory of Molecular Growth Regulation
National Institute of Child Health and Human Development
National Institutes of Health
Bethesda, Maryland 20892
[3]Program in Molecular Biology and Cancer
Samuel Lunenfeld Research Institute
Mount Sinai Hospital
600 University Avenue
Toronto, Ontario M5G 1X5
Canada
[4]Department of Molecular and Medical Genetics
University of Toronto
Toronto, Ontario M5S 1A8
Canada

Summary

The antiviral protein kinase PKR inhibits protein synthesis by phosphorylating the translation initiation factor eIF2α on Ser51. Binding of double-stranded RNA to the regulatory domains of PKR promotes dimerization, autophosphorylation, and the functional activation of the kinase. Herein, we identify mutations that activate PKR in the absence of its regulatory domains and map the mutations to a recently identified dimerization surface on the kinase catalytic domain. Mutations of other residues on this surface block PKR autophosphorylation and eIF2α phosphorylation, while mutating Thr446, an autophosphorylation site within the catalytic-domain activation segment, impairs eIF2α phosphorylation and viral pseudosubstrate binding. Mutational analysis of catalytic-domain residues preferentially conserved in the eIF2α kinase family identifies helix αG as critical for the specific recognition of eIF2α. We propose an ordered mechanism of PKR activation in which catalytic-domain dimerization triggers Thr446 autophosphorylation and specific eIF2α substrate recognition.

Introduction

The protein kinases PKR, HRI, PERK, and GCN2, which constitute a functional family called the eIF2α protein kinases, share a conserved kinase domain (KD); however, unique regulatory domains enable PKR to respond to viral infection, HRI to heme deficiency, PERK to endoplasmic reticulum stress, and GCN2 to amino acid limitation (Dever, 2002). All four kinases specifically phosphorylate Ser51 on the α subunit of the translation initiation factor eIF2, a GTP binding protein that delivers the initiator methionyl-tRNA to the small ribosomal subunit in the first step of translation initiation. Phosphorylation of eIF2α converts eIF2 from a substrate to an inhibitor of its GDP-GTP exchange factor eIF2B, thereby blocking protein synthesis (Hinnebusch, 2000).

PKR is a component in the cellular antiviral defense mechanism. Expression of PKR is transcriptionally induced by interferon, and the kinase is activated upon binding to double-stranded RNA (dsRNA). Human PKR consists of 551 amino acids, with the KD in the C-terminal half (residues 258–551) of the protein. The N-terminal regulatory region of PKR consists of two dsRNA binding domains (dsRBDs). PKR is thought to exist in cells in a latent monomeric state in which the dsRBDs may autoinhibit the kinase (Langland and Jacobs, 1992; Nanduri et al., 2000; Wu and Kaufman, 1997). Accordingly, binding of dsRNA to the dsRBDs causes a conformational change in PKR that disrupts this inhibitory interaction.

It is well established that the dsRBDs function to promote dimerization of PKR through binding dsRNA, as mutations that disrupt dsRNA binding interfere with dimerization and impair PKR autophosphorylation and substrate phosphorylation (Carpick et al., 1997; Cosentino et al., 1995; Romano et al., 1995; Zhang et al., 2001). Studies demonstrating that heterologous dimerization domains functionally substitute for the dsRBDs in PKR underscore the importance of dimerization for PKR function. Whereas the PKR-KD inefficiently phosphorylates eIF2α in vitro or when expressed in yeast or mammalian cells, fusion of the heterologous dimerization domain from glutathione S-transferase (GST) to the PKR-KD restores eIF2α phosphorylation both in vitro and in vivo (Dar and Sicheri, 2002; Ung et al., 2001).

A large number of autophosphorylation sites have been reported on PKR; however, the most compelling evidence for functional relevance has been reported for the KD activation-segment residue Thr446. Autophosphorylation on this site has been demonstrated using mass spectrometry analysis of PKR expressed in yeast and by using phospho-Thr446-specific antibodies to detect native PKR in mammalian cells treated with dsRNA (Romano et al., 1998; Zhang et al., 2001). High-level expression of human PKR, but not catalytically dead PKR-K296R, is lethal in yeast due to severe inhibition of translation initiation, and this toxicity is suppressed in cells expressing nonphosphorylatable eIF2α-S51A in which the Ser51 phosphorylation site is substituted by Ala (Chong et al., 1992; Dever et al., 1993). Similarly, substitution of Ala for Thr446 in PKR significantly weakens PKR toxicity in yeast and impairs autophosphorylation and eIF2α phosphorylation by immunopurified PKR (Romano et al., 1998).

PKR has been implicated in cellular growth control and a number of cell signaling pathways; however, it is unclear whether these PKR activities are mediated through phosphorylation of eIF2α or additional substrates. The vaccinia virus K3L protein is a pseudosubstrate inhibitor of PKR. K3L and eIF2α share a β barrel fold originally identified in the ribosomal protein S1 (Dar and Sicheri, 2002; Dhaliwal and Hoffman, 2003; Nonato

*Correspondence: tdever@nih.gov

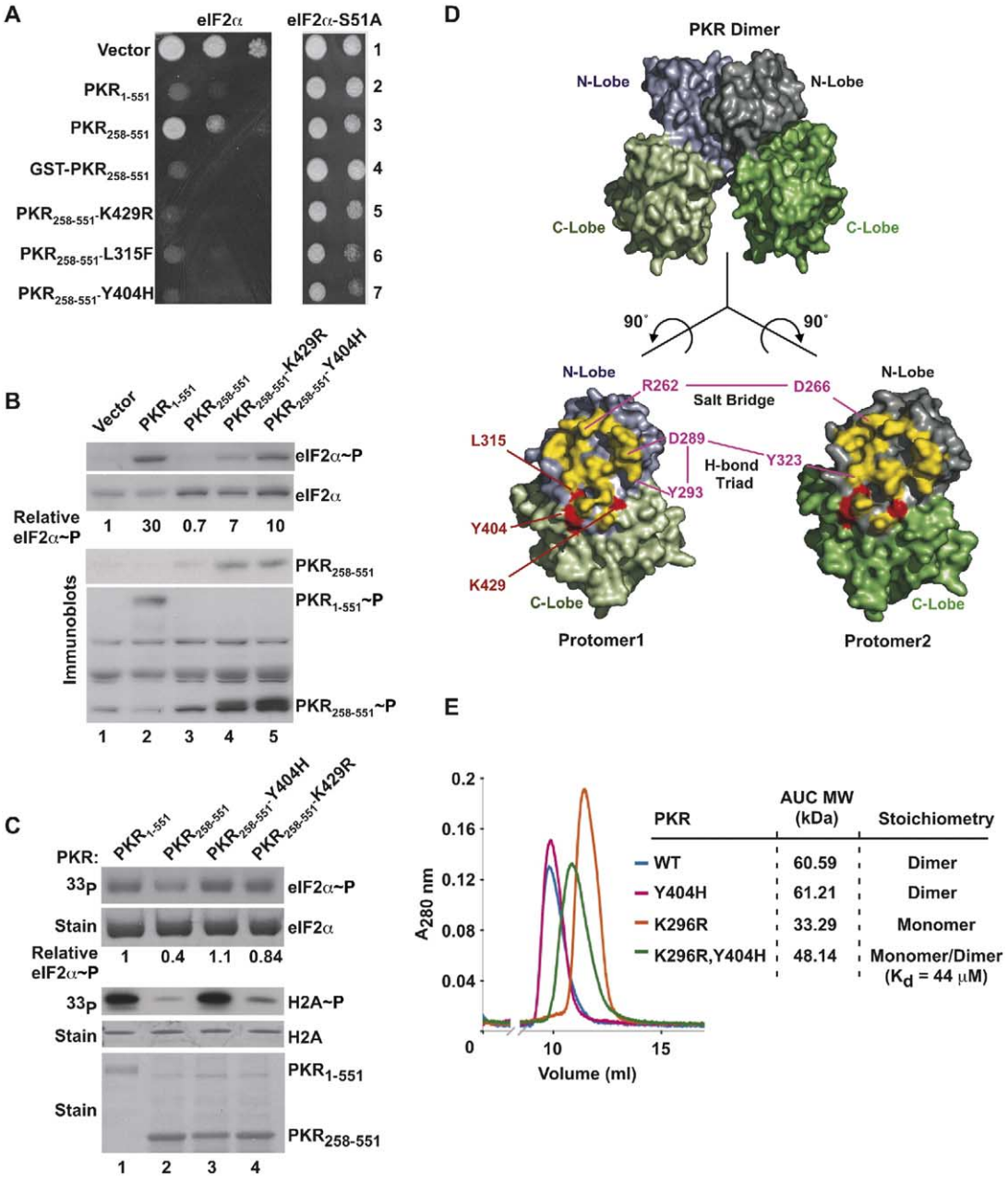

Figure 1. Identification of Mutations that Activate the PKR Catalytic Domain

(A) Activating mutations enhance PKR toxicity in yeast. Plasmids expressing full-length $PKR_{1–551}$; the KD only ($PKR_{258–551}$); the KD fused to GST (GST-$PKR_{258–551}$); the KD containing the mutations L315F, Y404H, or K429R, as indicated; or empty vector were introduced into yeast strains H2557 (eIF2α) and J223 (eIF2α-S51A), as indicated. Transformants were grown to saturation, and 4 μl of serial dilutions (of OD_{600} = 1.0, 0.1, 0.01) were spotted on minimal SGal medium and incubated 3 days at 30°C.

(B) Immunoblot analysis of PKR and eIF2α phosphorylation. WCEs were prepared from yeast transformants described in (A) and then subjected to SDS-PAGE followed by immunoblot analysis using phosphospecific antibodies against Ser51 in eIF2α (top panel) or Thr446 in PKR (bottom panel). The membrane was then stripped and probed using polyclonal antisera against yeast eIF2α (second panel) or poly-His tag to detect $PKR_{258–551}$ (third panel), as indicated. The relative level of eIF2α phosphorylation as determined by quantitative densitometry is indicated.

(C) In vitro protein-kinase assays. wt PKR or the indicated $PKR_{258–551}$ mutants were purified from yeast and mixed with [γ-^{33}P]ATP and recombinant GST-eIF2α (top two panels) or histone H2A (third and fourth panels). Kinase reactions were resolved on SDS-PAGE, stained with Coomassie blue (second and fourth panels), and subjected to autoradiography to visualize phosphorylated eIF2α (eIF2α~P, top panel) or phosphorylated H2A (H2A~P, third panel). The relative level of eIF2α phosphorylation as determined by quantitative densitometry is indicated. (Bottom panel) Equimolar amounts of the PKR stocks used for the kinase assays were resolved on SDS-PAGE and stained with Coomassie blue.

(D) Surface representation of the PKR dimer. (Top) Lateral perspective of the PKR catalytic-domain dimer. The left protomer is colored purple and light green, and the right protomer is colored gray and dark green for N and C lobes, respectively. (Bottom) The catalytic-domain dimer

et al., 2002). The PKR recognition determinants on K3L and eIF2α have been mapped to a conserved surface remote from the Ser51 phosphorylation site in eIF2α. Mutations of residues on this conserved surface of K3L disrupt binding and block inhibition of PKR (Dar and Sicheri, 2002; Kawagishi-Kobayashi et al., 1997). Likewise, mutations of the corresponding residues in eIF2α prevent Ser51 phosphorylation by both PKR and GCN2 (Dey et al., 2005). The importance of this conserved surface on eIF2α for PKR recognition, combined with the fact that PKR inefficiently phosphorylates peptides derived from the eIF2α sequences flanking Ser51 (Mellor and Proud, 1991), led to a model in which the PKR-KD binds tightly to the conserved surface on eIF2α to position the Ser51 phosphoacceptor toward the kinase active site (Dey et al., 2005). This model suggests that PKR elements remote from the active site will play critical roles in eIF2α recognition. However, residues in PKR that mediate eIF2α-specific substrate recognition have not been identified.

To gain additional insights into the mechanism of PKR activation and substrate recognition, and to test predictions based on our recently determined structure of PKR bound to eIF2α (Dar et al., 2005), we conducted a mutational and biochemical analysis of PKR. Our results define an ordered pathway of PKR activation in which KD dimerization is required for activation-segment autophosphorylation, which in turn is essential for specific eIF2α substrate recognition. Our results also reveal a link between Thr446 activation-segment phosphorylation and both dimerization and the ability to recognize eIF2α and K3L.

Results

Isolation of Mutations in PKR that Activate the Catalytic Domain in the Absence of an Extrinsic Dimerization Domain

High-level expression of full-length human PKR (residues 1–551) from a galactose-inducible promoter inhibited yeast cell growth (Figure 1A, row 2: $PKR_{1–551}$) due to high-level eIF2α phosphorylation (Figure 1B, lane 2). In contrast to full-length PKR where the N-terminal dsRBDs promote KD (residues 258–551) dimerization through the ability to bind dsRNA in yeast, expression of the isolated PKR-KD in yeast did not inhibit cell growth or enhance eIF2α phosphorylation (Figure 1A, row 3 and Figure 1B, top panel, lane 3: $PKR_{258–551}$). Likewise, in vitro, the isolated PKR-KD inefficiently phosphorylated recombinant eIF2α on Ser51 (Figure 1C, top panel, lane 2). Fusing the constitutive dimer GST to the PKR-KD inhibited yeast cell growth (Figure 1A, row 4: GST-$PKR_{258–551}$). To gain further insights into the role of dimerization for PKR activation, we randomly mutated the PKR-KD and screened for mutants that were toxic in yeast in the absence of an extrinsic dimerization domain. As detailed in the Experimental Procedures, three mutants were isolated: $PKR_{258–551}$-L315F, $PKR_{258–551}$-Y404H, and $PKR_{258–551}$-K429R (Figure 1A, rows 5–7).

The toxic phenotypes observed when expressing these PKR mutants in yeast could be due to enhanced eIF2α phosphorylation or to promiscuous phosphorylation impairing the function of other cellular proteins critical for growth. Western analyses revealed enhanced Ser51 phosphorylation in the strains expressing full-length PKR or the $PKR_{258–551}$ mutants (Figure 1B, top panel, lanes 2, 4, and 5). In addition, whereas $PKR_{258–551}$ inefficiently phosphorylated eIF2α and the nonspecific substrate histone H2A in vitro, the Y404H and K429R mutations significantly enhanced kinase activity (Figure 1C, third panel). Importantly, the toxic phenotypes associated with expression of these PKR mutants as well as GST-PKR and wild-type (wt) full-length PKR were suppressed in a yeast strain expressing nonphosphorylatable eIF2α-S51A (Figure 1A, rows 5–7), indicating that promiscuous phosphorylation of other proteins did not significantly contribute to the impaired growth of the strains expressing the PKR mutants. Taken together, these results demonstrate that the Y404H and K429R mutations bypass the requirement for an extrinsic dimerization domain and enhance the eIF2α kinase activity of the PKR-KD.

In the crystal structures of PKR bound to eIF2α, it is noteworthy that a large conserved surface of the protein-kinase N-terminal lobe is buried in an intermolecular dimer interface. Strikingly, all three PKR mutations isolated to activate $PKR_{258–551}$ map directly to this dimer interface (Figure 1D). Based on this location, we hypothesized that the PKR mutations enhance dimerization of the isolated PKR-KD and thereby bypass the requirement for an extrinsic dimerization domain or dispose with the need for dimerization altogether. To investigate this issue further, we used gel filtration chromatography and analytical ultracentrifugation to analyze PKR-KD dimerization. Whereas wt PKR-KD behaved as a dimer in these assays, catalytically dead KD-K296R was clearly monomeric (Figure 1E). Interestingly, the PKR-KD-K296R,Y404H double mutant was in a monomer-dimer equilibrium in these assays, with an average molecular weight ~1.5 times the size of a PKR-KD monomer (Figure 1E). In addition, whereas the K296R mutation abolished the interaction of the PKR-KD with itself in yeast two-hybrid assays, the Y404H

has been separated and rotated 90° about the vertical axis in opposite directions, as indicated, to reveal the interaction surfaces. Dimer-interface residues are highlighted in yellow. The intermolecular salt bridge between Arg262 and Asp266 and the H bond triad among Tyr293, Asp289, and Tyr323 are labeled. For clarity, the residues that form the identical reciprocal interactions have not been highlighted. Sites of mutations identified to activate the PKR catalytic domain in the absence of an extrinsic dimerization domain are colored red.

(E) Y404H mutation enhances PKR-KD dimerization. Gel filtration elution profiles from the application of wt and mutant PKR-KD on a Superdex-75 gel filtration column (24 ml bed volume) are shown. The column was pre-equilibrated in 150 mM NaCl, 10 mM HEPES (pH 7.5), and 3 mM DTT, and chromatograms correspond to the injection of 1.5–3.0 mg of protein. Molecular-weight values were determined using equilibrium sedimentation analytical ultracentrifugation (AUC, see Experimental Procedures). Global self-association analyses of the samples were performed separately to derive the apparent molecular weights, and the stoichiometry was inferred from the theoretical molecular weight (32,660 Da based on protein sequence) of the PKR-KD monomer.

and K429R mutations enhanced the PKR-KD yeast two-hybrid interaction (see below). Thus, we conclude that the PKR-activating mutations promote catalytic-domain dimerization and bypass the normal requirement for dimerization mediated by the PKR dsRBDs.

Mutations in the PKR Dimer Interface Impair Kinase Autophosphorylation and Substrate Phosphorylation

The structural analysis of PKR (Dar et al., 2005) identified two prominent sets of intermolecular interactions at the dimer interface involving residues conserved among all eIF2α kinases. A salt bridge was evident between Arg262 in one PKR protomer and Asp266 in the second protomer, while Asp289 and Tyr293 in one protomer and Tyr323 in the second protomer form a hydrogen-bonding (H bond) triad (Figure 1D). To test the importance of these interactions, we mutated these residues in full-length PKR and examined PKR toxicity in a *gcn3-102* yeast strain containing a mutation in the α subunit of eIF2B that partially desensitizes eIF2B to inhibition by phosphorylated eIF2 (Dever et al., 1993). Whereas expression of full-length PKR is lethal in wt yeast (Figure 1A, row 2), a slow-growth phenotype is observed in the *gcn3-102* strain (Figure 2A, row 1) (see also Figure S2 in the Supplemental Data available with this article online).

To test the importance of the predicted salt bridge between residues Arg262 and Asp266, these residues were mutated individually and together to Asp and Arg, respectively. Single mutations of both R262D and D266R, which are predicted to disrupt the salt bridge, suppressed PKR toxicity and lowered eIF2α phosphorylation in yeast (Figure 2A, rows 3–4 and Figure 2B, third panel, lanes 3 and 4), though not as completely as the kinase-dead K296R mutation (Figures 2A and 2B, lane 2). Importantly, combining the two mutations in PKR-R262D,D266R, which is predicted to re-establish the salt bridge interaction with opposite polarity, restored PKR toxicity and eIF2α phosphorylation in yeast (Figure 2A, row 5 and Figure 2B, third panel, lane 5).

Autophosphorylation of PKR on Thr446 in the activation segment has been correlated with PKR activity (Romano et al., 1998; Zhang et al., 2001), and, in the PKR crystal structures, this is the only residue observed to be stoichiometrically phosphorylated (Dar et al., 2005 [this issue of *Cell*]). Whereas wt PKR expressed in yeast was readily detected using phospho-Thr446 antibodies, catalytically dead PKR-K296R was not detected (Figure 2B, top panel, lanes 1 and 2), demonstrating that Thr446 phosphorylation is mediated by PKR and not by an endogenous yeast kinase. The D266R and R262D mutations either partially or almost completely eliminated, respectively, Thr446 phosphorylation (Figure 2B, top panel, lanes 3 and 4). However, the mutations did not impair PKR expression (Figure 2B, second panel). Consistent with the notion that PKR dimerization is required for autophosphorylation, the R262D,D266R double mutation, which is predicted to re-establish the salt bridge, as well as the K429R and Y404H mutations, which activated $PKR_{258–551}$ in the absence of an extrinsic dimerization domain, restored PKR phosphorylation on Thr446 (Figure 2B, lane 5 and Figure 1B, bottom panel, lanes 4 and 5).

Next we examined the importance of the predicted H bond triad composed of residues Asp289, Tyr293, and Tyr323 by mutating each residue to Ala. The D289A and Y323A mutations significantly reduced PKR toxicity in yeast (Figure 2A, rows 6 and 8) and either lowered or practically eliminated PKR autophosphorylation and eIF2α phosphorylation, respectively (Figure 2B, lanes 6 and 8 and Figure S4C). Combining the D289A and Y293A mutations resulted in a more significant impairment of PKR function in yeast (Figures 2A and 2B, lane 9), and, like catalytically dead PKR-K296R, PKR-D289A,Y293A failed to autophosphorylate or phosphorylate either specific (eIF2α) or nonspecific (histone H2A) substrates in vitro (Figure 2C, lane 4 and Figure 2D, lane 3). Trp327, which forms a close van der Waals contact with the aliphatic portion of the Arg262 side chain within the salt bridge, is perfectly conserved among all eIF2α kinases (Figure S1). Whereas substitution of Trp327 by an aromatic residue retained PKR toxicity in yeast and PKR kinase activity in vitro (Figures 2A and 2B, row 10 and Figure 2C, lane 5), all other substitutions including Ala and Leu abolished PKR toxicity (Figure 2A, rows 10–12 and Figure S5) and impaired PKR autophosphorylation and eIF2α phosphorylation both in vivo (Figure 2B, lanes 11 and 12) and in vitro (Figure 2C, lane 6).

Having identified the Y404H and K429R mutations as activating PKR lacking an extrinsic dimerization domain (Figure 1A), we asked if these mutations could bypass the requirement for the salt bridge between Arg262 and Asp266 in PKR. Whereas the Y404H and K429R mutations did not hyperactivate full-length PKR (which is already very active and toxic, Figure S4A), introduction of these dimer bypass mutations into PKR-D266R restored PKR toxicity (Figure 3A, rows 4–6 and Figure S4B), PKR autophosphorylation, and eIF2α phosphorylation in yeast (Figure 3B, lanes 4–6). Together with the results on the Trp327 and H bond-triad mutagenesis, the ability of the Y404H and K429R dimer-interface mutations to compensate for the lost salt-bridge interaction between Arg262 and Asp266 provides strong evidence that a proper PKR dimer configuration is required for kinase autophosphorylation and efficient substrate phosphorylation.

As described earlier, the PKR-KD (residues 238–551) readily interacts with itself in yeast two-hybrid assays (Figure 3C), consistent with our analytical ultracentrifugation studies (Figure 1E). The R262D, D266R, and Y323A single mutations as well as the D289A,Y293A double mutation blocked the PKR-KD two-hybrid interaction (Figure 3C). In contrast, engineering the complementing R262D and D266R mutations into the two-hybrid activation-domain and binding-domain fusions, respectively, restored the two-hybrid interaction. These data provide direct support for the idea that the salt bridge and H bond-triad interactions are critical for PKR-KD dimerization and the promotion of activation-segment autophosphorylation.

PKR Autophosphorylation on the Activation-Segment Residue Thr446 Enhances Specific eIF2α Recognition

Previously it was reported that mutation of the Thr446 autophosphorylation site significantly impaired PKR

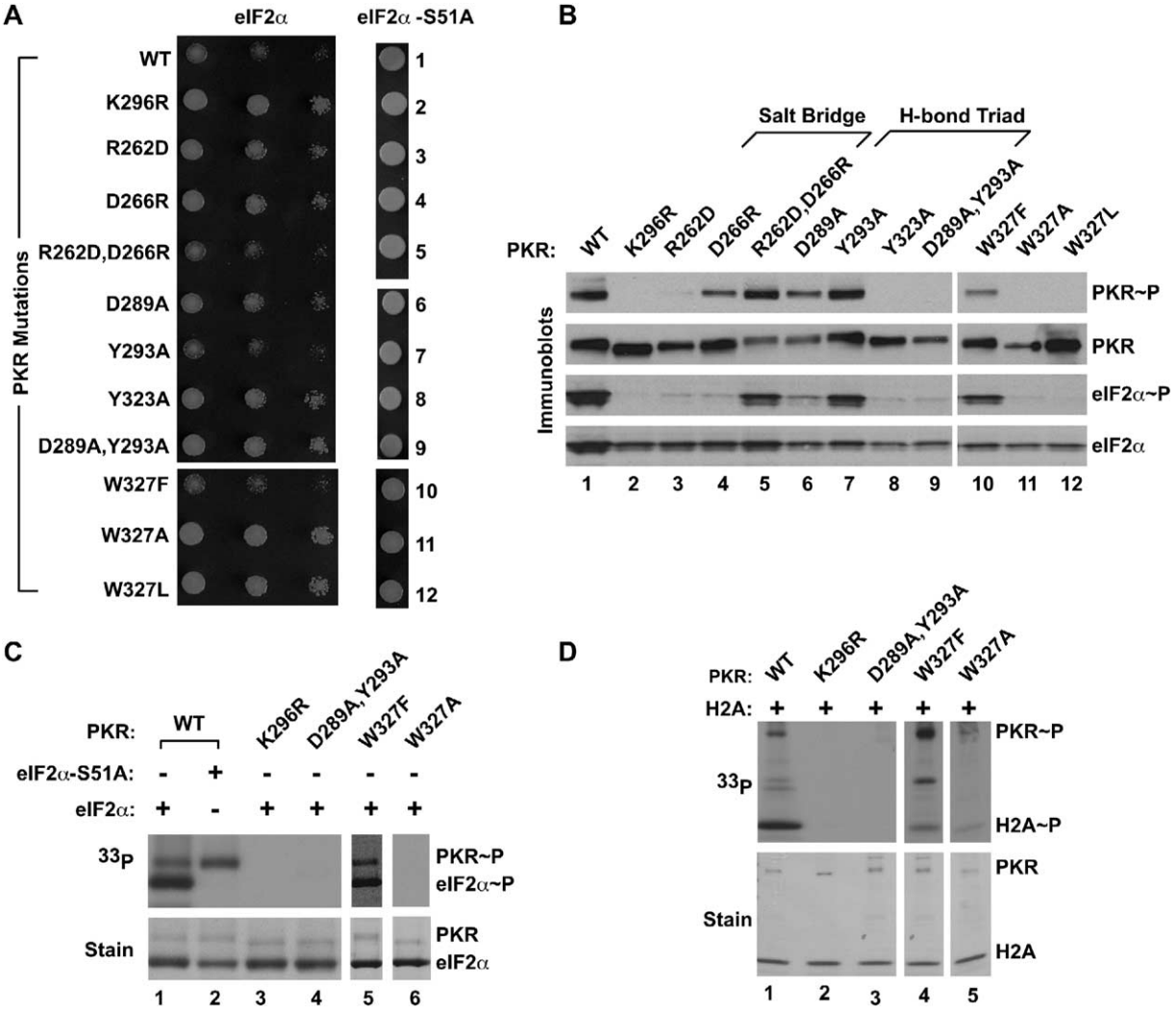

Figure 2. Mutations in the PKR Dimer Interface Impair Autophosphorylation and eIF2α Phosphorylation

(A) Mutations in the dimer interface reduce PKR toxicity in yeast. Plasmids expressing wt or the indicated $PKR_{1–551}$ mutants were introduced into strains H17 (eIF2α) and J82 (eIF2α-S51A). Transformants were grown and serial dilutions were spotted as described in Figure 1A.

(B) Mutations at the PKR dimer interface impair autophosphorylation and eIF2α phosphorylation in vivo. WCEs were prepared from H17 transformants described in (A) and then subjected to immunoblot analysis using antibodies to detect phospho-Ser51 in eIF2α (third panel), total eIF2α (bottom panel), phospho-Thr446 in PKR (top panel), and total PKR (second panel).

(C and D) Mutations at the PKR dimer interface impair autophosphorylation and eIF2α and histone phosphorylation in vitro. wt or the indicated PKR mutants were purified from yeast and mixed with [γ-^{33}P]ATP and recombinant GST-eIF2α or GST-eIF2α-S51A (C) or recombinant H2A (D). Kinase reactions were resolved on SDS-PAGE, stained with Coomassie blue (lower panels), and subjected to autoradiography to visualize phosphorylated PKR (PKR∼P), eIF2α (eIF2α∼P), and histone H2A (H2A∼P).

function in yeast (Romano et al., 1998; Zhang et al., 2001). Using the more sensitive eIF2Bα mutant yeast strain, we found that PKR-T446A, like catalytically dead PKR-K296R, did not inhibit yeast cell growth (Figure 4A). Consistent with this lack of growth phenotype, practically no eIF2α Ser51 phosphorylation was detected in strains expressing PKR-T446A (Figure 4B), and, in in vitro kinase assays, PKR-T446A was defective for incorporation of phosphate into either itself or eIF2α (Figure 4C, lanes 3–5).

In addition, kinetic analyses revealed that wt PKR was over 40-fold more active at phosphorylating the nonspecific substrate histone H2A than PKR-T446A was (Figure 4D), though the K_M for the reaction was nearly identical for the two kinases (Figure 4D). These results, combined with the fact that the T446A mutation impaired eIF2α phosphorylation to a greater extent than it impaired histone phosphorylation, indicate that PKR autophosphorylation on Thr446 is important for PKR catalytic efficiency and specific (eIF2α) substrate recognition but not for recognition of nonspecific substrates.

To gain further insight into the importance of PKR autophosphorylation for specific substrate recognition, we used surface plasmon resonance (SPR) to examine the binding of wt and mutant forms of PKR to the vac-

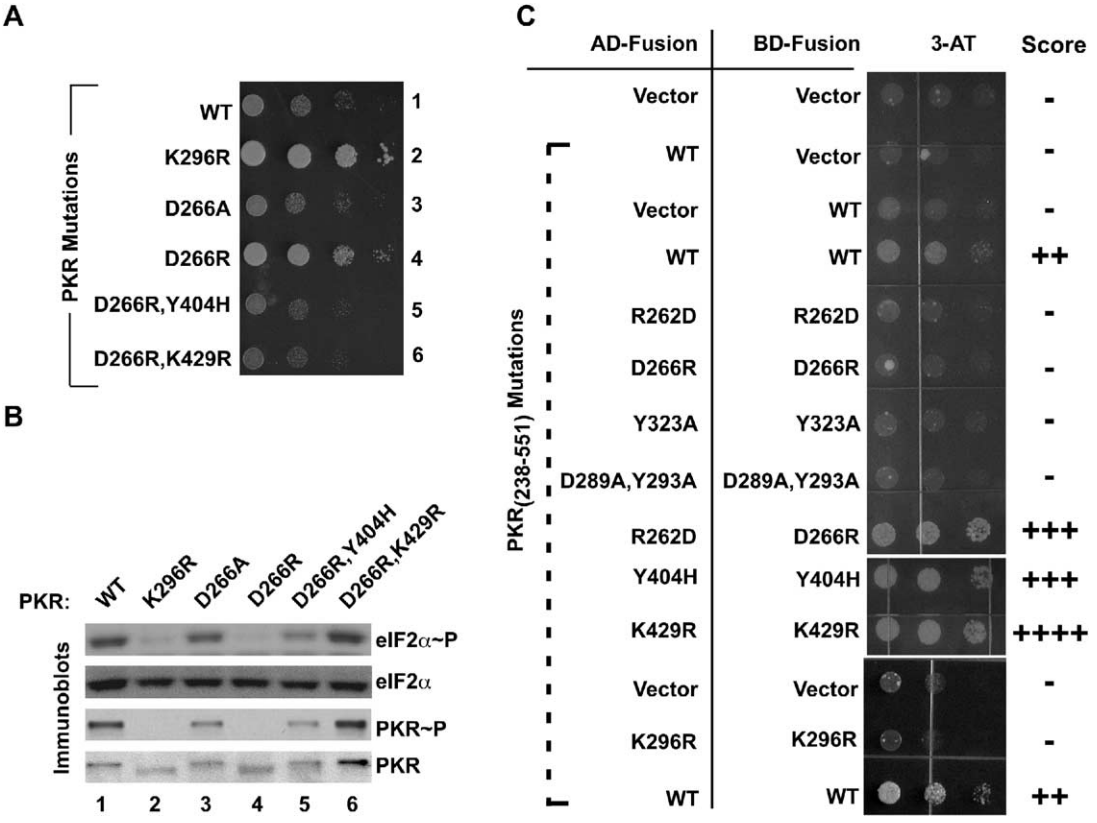

Figure 3. Functional Complementation of a PKR Dimer-Interface Mutation by Mutations that Activate the PKR Catalytic Domain

(A) Combining PKR-activating mutations with the dimer-interface mutation restores PKR toxicity in yeast. Transformants of strain H17 expressing the indicated PKR mutants were grown and serial dilutions were spotted as described in Figure 1A.

(B) PKR-activating mutations restore autophosphorylation and eIF2α phosphorylation in yeast. WCEs were prepared from transformants described in (A) and analyzed as described in Figure 2B.

(C) PKR dimer-interface mutations impair KD interaction in the yeast two-hybrid assay. Plasmids expressing the indicated wt or mutant forms of $PKR_{238–551}$ fused to either the GAL4 DNA binding domain (BD-fusion, pGBT10 derivatives) or the GAL4 transcriptional activation domain (AD-fusion, pGAD425 derivatives) (Tan et al., 1998) were introduced into yeast strain Y190. Serial dilutions of transformants were spotted on synthetic medium containing 50 mM 3-aminotriazole (3-AT) and incubated 5 days at 30°C. Growth of transformants, indicating the degree of two-hybrid interaction, was scored and ranked from – (no growth, poor interaction) to ++++ (good growth, strong interaction).

cinia virus K3L protein, a pseudosubstrate inhibitor of PKR and molecular mimic of eIF2α. wt and T446A and K296R mutant versions of GST-PKR-KD and PKR-KD were tested for binding to immobilized K3L protein. Both dimeric GST-PKR-KD and the isolated PKR-KD liberated from GST by cleavage with TEV protease bound to immobilized K3L (Figure 4E, upper panels). However, the binding reactions displayed different kinetics (sigmoidal versus nonsigmoidal), with GST-PKR-KD binding well to K3L even at low kinase concentrations where the isolated PKR-KD bound poorly (Figure 4F). However, binding of isolated PKR-KD to K3L was recovered at higher kinase concentrations (Figure 4F). Interestingly, global fitting of the association and dissociation phases of the GST-PKR-KD and PKR-KD binding kinetics agrees best with a bivalent analyte model, suggesting that both GST-PKR-KD and PKR-KD bind K3L as preformed dimers (Figure S6B). This result is consistent with our analytical ultracentrifugation studies, which show that isolated wt PKR-KD is a dimer (Figure 1E). Under the conditions of the SPR experiments, PKR-KD-T446A and PKR-KD-K296R in both the presence and absence of the GST dimerization domain failed to show detectable binding to the K3L protein (Figure 4E and Figure S6A). All four forms of the latter proteins are free of phosphate on Thr446 either by virtue of the fact that the kinase is catalytically dead or the fact that the site is removed. Interestingly, the analytical ultracentrifugation studies in Figure 1E, as well as the two-hybrid experiments in Figure 3C, revealed that the K296R mutation that abolished PKR autophosphorylation likewise blocked KD dimerization. These results, combined with the results of the dimer-interface mutations (Figure 2) and SPR experiments, indicate that PKR dimerization and activation-segment phosphorylation on Thr446 together strongly influence the specific recognition of eIF2α substrate and K3L pseudosubstrate.

Conserved Residues on Helix αG are Important Determinants for Specific Substrate Recognition by the eIF2α Kinases

Comparison of amino acid sequence alignments of a sampling of eIF2α and unrelated protein-kinase domains identified 17 residues that were preferentially

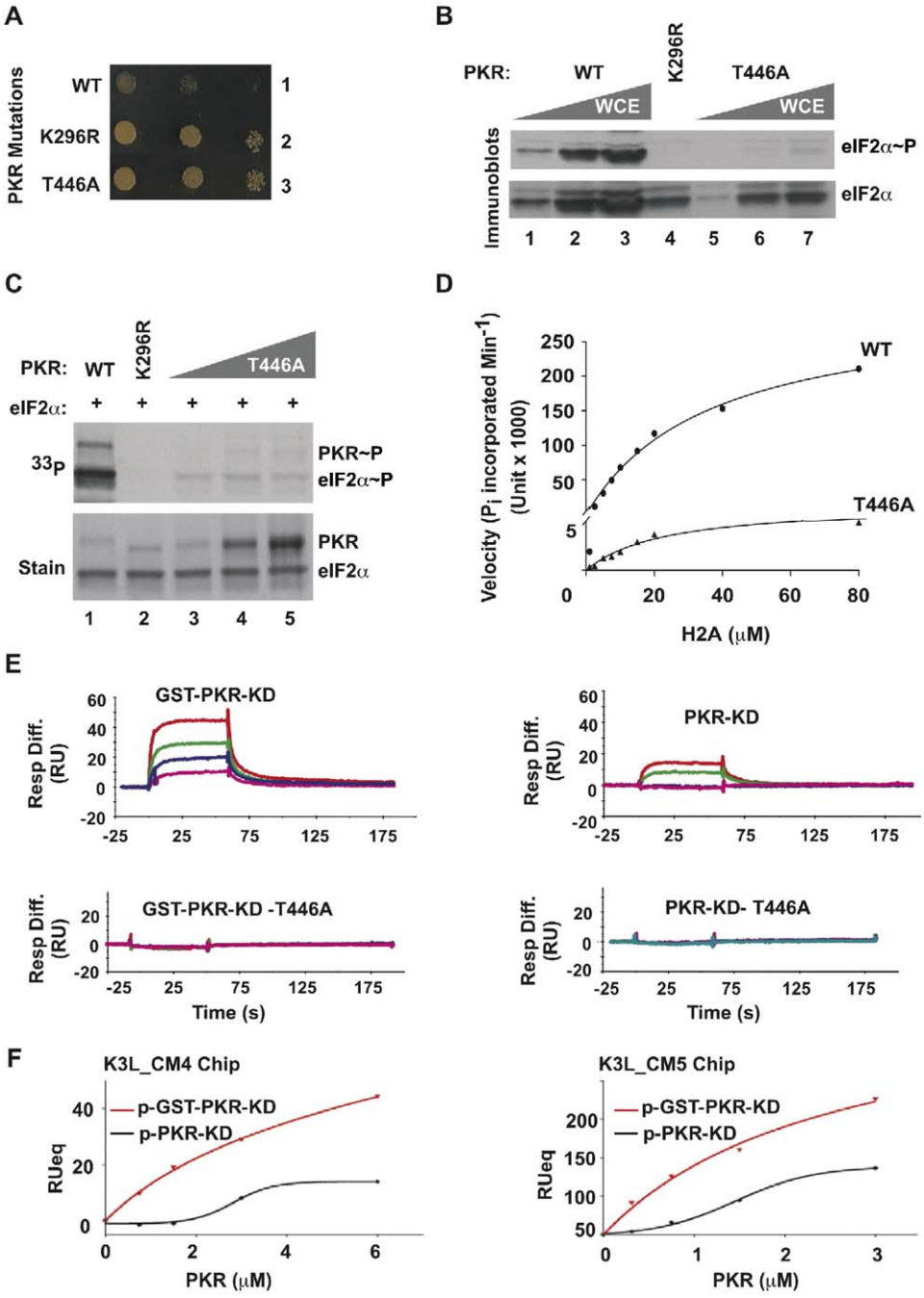

Figure 4. PKR Autophosphorylation on Activation-Loop Residue Thr446 Is Critical for Kinase Activity and eIF2α Recognition

(A) Substitution of Ala for Thr446 reduces PKR toxicity in yeast. Transformants of strain H17 expressing the indicated PKR mutants were grown and serial dilutions were spotted as described in Figure 1A.

(B) PKR-T446A mutation impairs eIF2α phosphorylation in yeast. WCEs were prepared from transformants described in (A), and then 1 μg, 5 μg, and 10 μg were subjected to immunoblot analysis using antibodies to detect phospho-Ser51 in eIF2α (top panel) and total eIF2α (bottom panel).

(C) PKR-T446A mutation impairs PKR autophosphorylation and eIF2α phosphorylation in vitro. wt or the indicated PKR mutants were purified from yeast and 0.2 μM PKR or PKR-K296R, and 0.2 μM, 1 μM, or 2 μM PKR-T446A were mixed with [γ-^{33}P]ATP and recombinant GST-eIF2α. Kinase reactions were resolved on SDS-PAGE, stained with Coomassie blue (lower panel), and subjected to autoradiography to visualize phosphorylated PKR (PKR ~ P) and eIF2α (eIF2α ~ P).

(D) Kinetic analyses of histone H2A phosphorylation by PKR and PKR-T446A. In vitro kinase assays containing 5 nM PKR or PKR-T446A and the indicated concentrations of recombinant histone H2A were resolved by SDS-PAGE. The relative incorporation of phosphate into H2A was determined by phosphorimage analysis, and the data are presented using arbitrary units.

(E) Effect of PKR dimerization and Thr446 activation-segment phosphorylation on binding to K3L. Isolated PKR-KD or GST fused PKR-KD (GST-PKR-KD), with or without Thr446 phosphorylation (T446A), were applied to a K3L amine-coupled CM4 chip at 0.75, 1.5, 3.0 and 6.0 μM concentrations (pink, blue, green, and red curves in each sensorgram, respectively), as described in Supplemental Data.

(F) Binding between K3L and phospho-PKR-KD, but not phospho-GST-PKR-KD, is sigmoidal with respect to protein-kinase concentration. Response units at equilibrium (RUeq) from the application of phospho-GST-PKR-KD and phospho-PKR-KD to K3L immobilized on CM4 (left) and at higher density on CM5 (right) chips are plotted as a function of protein-kinase concentration. RUeq is derived from the steady-state plateau of the association phases of the sensorgrams shown in (E).

conserved among the family of eIF2α protein kinases (Figure S1 and Dar et al., 2005). We reasoned that these conserved residues play roles in eIF2α kinase-specific functions such as kinase-domain dimerization and eIF2α recognition. To identify the PKR residues that mediate specific eIF2α recognition, we mutated each of the preferentially conserved residues and screened for loss of PKR toxicity in yeast. In addition to the dimer-interface residues and the Thr446 autophosphorylation site, mutations at residues Thr487 and Phe495 eliminated PKR toxicity in yeast (Figure 5A and Figures S2 and S3). Interestingly, both Thr487 and Phe495 reside on helix αG of the KD (Figure 6A). As revealed in the PKR•eIF2α crystal structure, helix αG adopts a novel conformation in PKR relative to all other protein-kinase structures determined to date (see Figure 4A in Dar et al., 2005) and composes a major portion of the binding surface with eIF2α (Figure 6A).

Substitution of Lys, Ala, or Asp for Thr487 eliminated eIF2α phosphorylation and abolished PKR toxicity in yeast (Figures 5A and 5B). Importantly, these mutations did not impair PKR expression or autophosphorylation on Thr446 in vivo (Figure 5B, top two panels). Further mutational analyses of Thr487 indicated that only the conservative substitution of Ser retained normal PKR activity (Figure S7A). Consistent with the in vivo results, PKR-T487K, PKR-T487A, and PKR-T487D were severely impaired for eIF2α phosphorylation in vitro, yet the kinases were efficiently autophosphorylated (Figure 5C and Figure S7B). As noted previously, PKR phosphorylates intact eIF2α ~1000-fold more efficiently than an eIF2α peptide substrate (Mellor and Proud, 1991; M.D., unpublished data), indicating that eIF2α recognition is driven by contacts remote from the phosphorylation site. The eIF2α model peptide and histone H2A likely only contact the phosphoacceptor binding site in PKR, and, thus, phosphorylation of these model substrates is a good indicator of intrinsic PKR catalytic efficiency. All three Thr487 mutants phosphorylated a peptide containing Ser51 but not the same peptide containing the S51A mutation (Figure 6B, top and middle panels and Figure S8). Likewise, all three PKR Thr487 mutants retained histone phosphorylation activity (Figure 6B, bottom panel and Figure S8A). Kinetic analyses revealed that the PKR-T487A and PKR-T487D mutations did not significantly impact the K_M for peptide or histone phosphorylation (Figures 6C and 6D). Thus, mutation of residue Thr487 does not impair general PKR kinase activity but rather specifically impairs phosphorylation of intact eIF2α. Based on these findings, we conclude that Thr487 is a key determinant of eIF2α-specific substrate recognition.

Like the Thr487 mutations, substitution of Arg, Ile, or Pro for Phe495 eliminated eIF2α phosphorylation and PKR toxicity in yeast (Figures 5A and 5B) but did not affect PKR expression or autophosphorylation on Thr446 (Figure 5B). Consistent with these in vivo results, PKR-F495P failed to phosphorylate eIF2α in vitro (Figure 5C) but retained eIF2α peptide and at least some histone phosphorylation activity (Figure 6B). Taken together, we conclude that residues Thr487 and Phe495 in helix αG play critical roles in the specific recognition of eIF2α by PKR.

The GCN2 kinase is required for induction of *GCN4* mRNA translation and growth of yeast cells under amino acid starvation conditions imposed by 3-AT (Hinnebusch, 2000). Whereas wt yeast grew on medium containing 3-AT, *gcn2Δ* cells expressing the kinase-dead subdomain II mutant GCN2-K628R failed to grow (Figure 5D, row 2). Substitution of Ala, Lys, or Asp for GCN2 residue Thr924, corresponding to PKR residue Thr487 (Figure S1), either partially or completely inhibited eIF2α Ser51 phosphorylation (Figure 5E, middle panel, lanes 3–5) and yeast cell growth in the presence of 3-AT (Figure 5D, rows 3–5). Importantly, the mutations did not impair GCN2 expression in yeast (Figure 5E, top panel) but blocked the ability of immunoprecipitated GCN2 to phosphorylate eIF2α in vitro (Figure 5F). In these in vitro kinase assays, it is noteworthy that the mutations (other than the kinase-dead *gcn2-K628R* mutation) did not impair GCN2 autophosphorylation (Figure 5F). Thus, mutation of the corresponding Thr in helix αG of both PKR and GCN2 severely impaired eIF2α phosphorylation.

Discussion

In mammalian cells, PKR is thought to exist in a latent form that is activated by binding to dsRNA generated during viral infection. Based on the results of the mutational studies reported here, previous mutational studies on PKR, and the X-ray crystal structure of a PKR•eIF2α complex (Dar et al., 2005), we propose a three-step pathway for PKR activation in which catalytic-domain dimerization facilitates activation-segment autophosphorylation, which in turn promotes the specific recognition of eIF2α substrate (Figure 7).

Role of Dimerization in PKR Catalytic Activation

Binding of dsRNA to the dsRBDs in the N-terminal regulatory region of PKR promotes dimerization of PKR and triggers autophosphorylation (Zhang et al., 2001). While PKR dimerization could simply increase the likelihood of autophosphorylation by bringing two molecules of PKR in close proximity (Lemaire et al., 2005), our data reveal the importance of a specific dimer orientation between the catalytic domains of two PKR molecules. Specifically, mutations that disrupt the salt bridge between Arg262 and Asp266 or the H bond triad between Asp289, Tyr293, and Tyr323 within the PKR dimer interface perturb kinase function both in yeast (Figure 2) and in mammalian cells (Figure S9) despite the presence of intact dsRBDs in the N-terminal regulatory region of PKR. As the N terminus of PKR dimerizes in the absence of the KD (Carpick et al., 1997; Cosentino et al., 1995; Ortega et al., 1996), it is reasonable to assume that disruption of the salt bridge or H bond triad does not impair the ability of full length PKR to dimerize. Thus, bringing two KDs in close proximity is not sufficient to promote catalytic activation of PKR. Rather, we propose that the loss of kinase function resulting from these mutations reveals the critical importance of the precise N lobe-to-N lobe dimer contact revealed in the PKR crystal structure. This notion is in accordance with previous genetic analyses revealing dominant-negative impacts of PKR-KD internal deletion mutants (Romano et al., 1995). Of note, a mutation

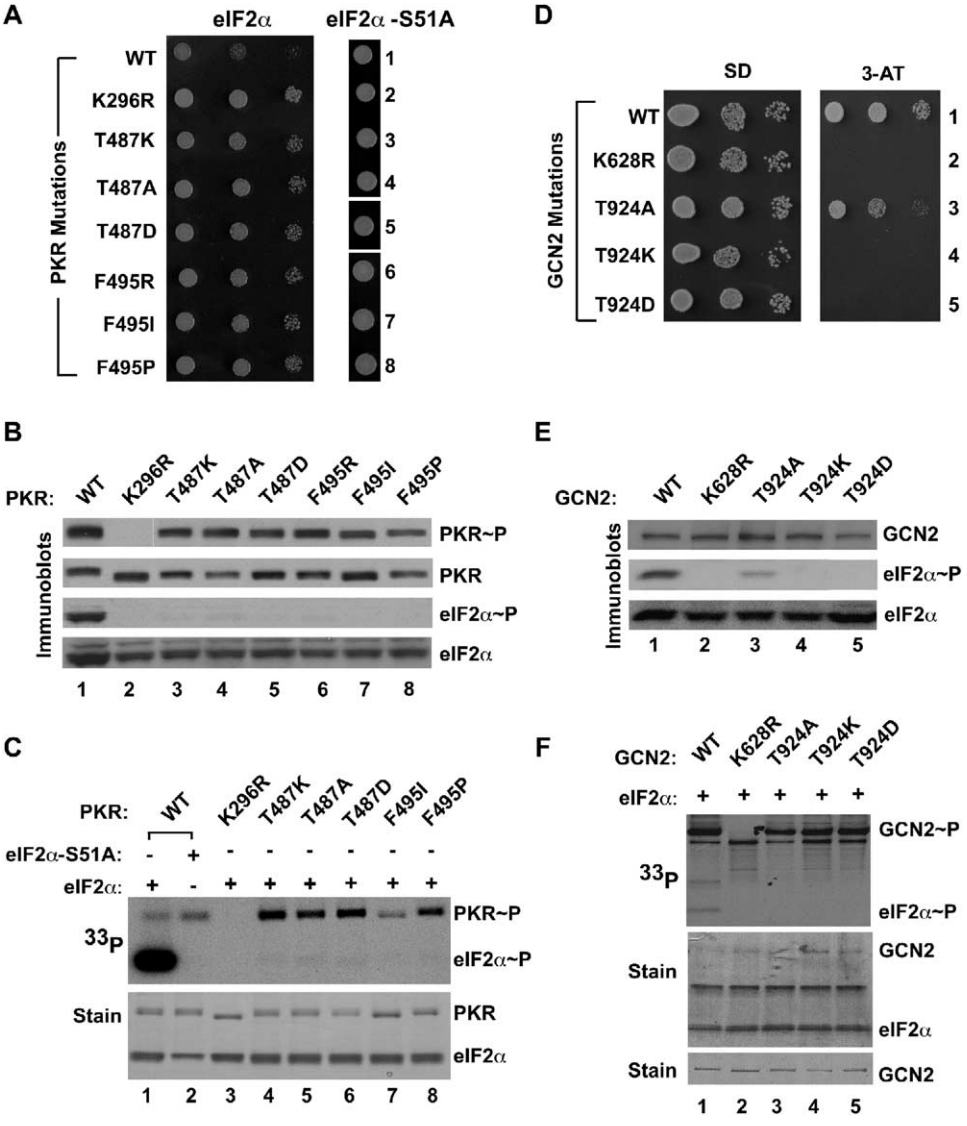

Figure 5. Conserved Thr in Helix αG of the Kinase Catalytic Domain Is Critical for eIF2α Recognition by PKR and GCN2

(A) Mutations at Thr487 and Phe495 reduce PKR toxicity in yeast. Plasmids expressing wt or the indicated PKR mutants were introduced into strains H17 (eIF2α) and J82 (eIF2α-S51A). Transformants were grown and serial dilutions were spotted as described in Figure 1A.

(B) Mutations at Thr487 and Phe495 impair eIF2α phosphorylation but not PKR autophosphorylation in yeast. WCEs of transformants described in (A) were prepared and analyzed as described in Figure 2B.

(C) Mutations at Thr487 and Phe495 impair eIF2α phosphorylation but not PKR autophosphorylation in vitro. wt or the indicated PKR mutants were purified from yeast and mixed with [γ-^{33}P]ATP and recombinant GST-eIF2α or GST-eIF2α-S51A. Kinase-reaction products were resolved on SDS-PAGE, stained with Coomassie blue (lower panel), and subjected to autoradiography to visualize phosphorylated PKR (PKR∼P) and eIF2α (eIF2α∼P).

(D) Analysis of substitutions at Thr924 on GCN2 function in vivo. Transformants of yeast strain H1894 expressing GCN2 or the indicated GCN2 mutants were grown to saturation, and 4 μl of serial dilutions (of OD_{600} = 1.0, 0.1, 0.01) were spotted on minimal SD medium or medium containing 3-AT. Plates were incubated 3 days at 30°C.

(E) Mutations at GCN2 residue Thr924 impair eIF2α phosphorylation in vivo. Transformants described in (D) were grown in SD medium and then supplemented with 10 mM 3-AT 1 hr prior to harvest. WCEs were subjected to immunoblot analysis to detect GCN2 (top panel), phosphorylated eIF2α (second panel), and total eIF2α (bottom panel).

(F) Thr924 mutations impair eIF2α phosphorylation but not GCN2 autophosphorylation in vitro. wt or the indicated GCN2 mutants were purified from yeast and mixed with [γ-^{33}P]ATP and recombinant yeast $eIF2\alpha_{1-200}$. Kinase-reaction products were resolved on SDS-PAGE, stained with Coomassie blue (middle panel; positions of GCN2 and eIF2α are indicated), and subjected to autoradiography (top panel) to visualize phosphorylated GCN2 (GCN2∼P) and eIF2α (eIF2α∼P). (Bottom panel) Equimolar amounts of the GCN2 stocks used for the kinase assays were resolved on SDS-PAGE and stained with Coomassie blue.

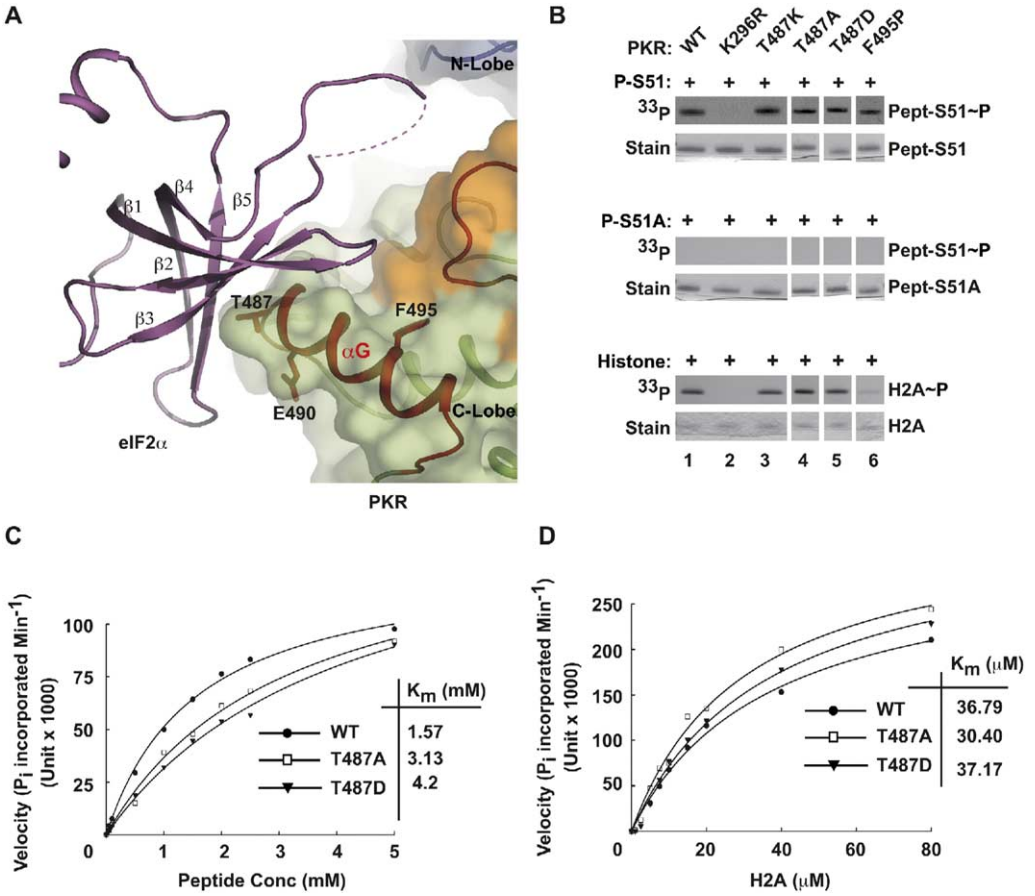

Figure 6. Mutations at the Conserved Thr in Helix αG of the Catalytic Domain Do Not Impair PKR Histone H2A or Peptide Phosphorylation Activities

(A) Ribbons representation of the PKR-eIF2α binding interface. eIF2α is shown in purple, while PKR, together with its transparent surface, is shown in green (C lobe), orange (activation segment), and blue (N lobe). Helix αG and residues tested for function are shown in red. Note: Glu490 mutations had no affect on PKR activity (see Figures S2 and S3).

(B) Peptide and histone phosphorylation assays. wt or the indicated PKR mutants were mixed with [γ-^{33}P]ATP and an eIF2$\alpha_{45–56}$ peptide (Pept-S51), the same peptide with Ser51 mutated to Ala (Pept-S51A), or recombinant H2A. Kinase reactions were resolved on Tricin peptide gels (peptide assays) or SDS-PAGE (H2A assays), stained with Coomassie blue (lower panels), and subjected to autoradiography to visualize phosphorylated peptide (Pept-S51 ~ P) and histone H2A (H2A ~ P).

(C and D) Kinetic analyses of peptide (C) and histone H2A (D) phosphorylation by PKR, PKR-T487A, and PKR-T487D. In vitro kinase assays containing 5 nM PKR, PKR-T487A, or PKR-T487D and the indicated concentrations of eIF2$\alpha_{45–56}$ peptide (Pept-S51, [C]) or recombinant histone H2A (D) were resolved by SDS-PAGE. The relative incorporation of phosphate into H2A was determined by phosphorimage analysis, and the data are presented using arbitrary units. Inset: K_M measurements were performed using KaleidaGraph.

substituting Gln for Arg587 in PERK, corresponding to Arg262 in PKR, was identified in a patient with Wolcott-Rallison syndrome, a rare form of diabetes (Delepine et al., 2000). Based on our studies of PKR, this mutation is likely to inactivate PERK by eliminating an intermolecular salt bridge and disrupting proper catalytic-domain dimerization and kinase activation.

Role of Thr446 Activation-Segment Phosphorylation on PKR Function

Thr446 within the activation segment of PKR was previously identified as a functionally relevant autophosphorylation site (Romano et al., 1998), and, while additional sites have been identified in the N-terminal regulatory region and the KD of PKR, mutation of these latter sites has little or no impact on PKR function (Zhang et al., 2001). Mutation of conserved dimer-interface residues blocked Thr446 phosphorylation (Figure 2B), and the Y404H and K429R activating mutations stimulated KD phosphorylation on Thr446 (Figure 1B), indicating that only a specific dimeric orientation of the catalytic domain is competent for transferring phosphate onto Thr446 (Figure 7). As shown here, the T446A mutation severely impaired the nonspecific phosphorylation of histones and nearly eliminated eIF2α phosphorylation. In addition, both the selective mutation of Thr446 to Ala and the K296R mutation that blocks all PKR autophosphorylation eliminated any detectable binding of GST-PKR-KD and the isolated PKR-KD to K3L (Figure 4E). Interestingly, the K296R mutation also impaired PKR-KD dimerization, indicating that catalytic-domain dimerization promotes activation-segment

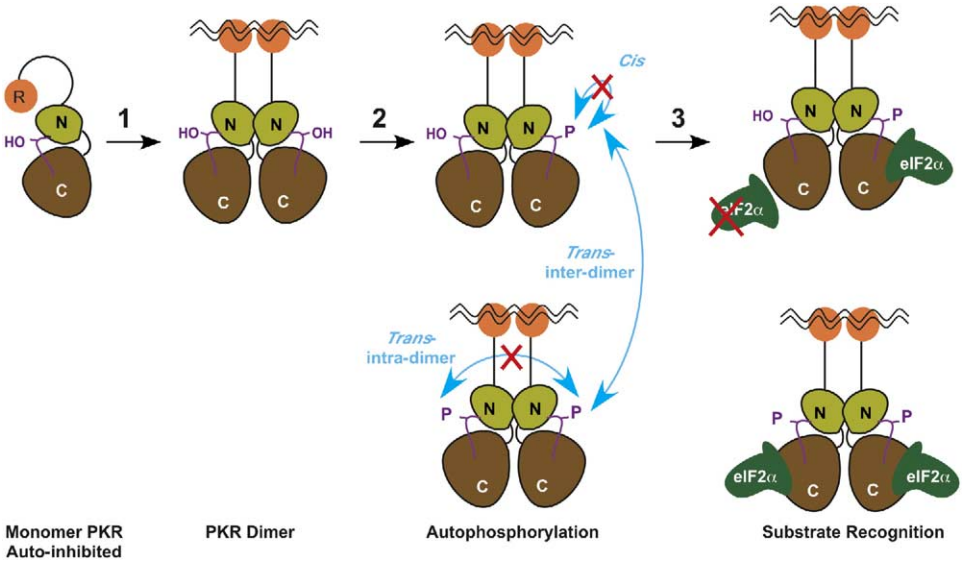

Figure 7. Model of PKR Activation Pathway: Dimerization-Dependent Autophosphorylation and eIF2α Substrate Recognition

In its monomeric state, PKR (KD N lobe is lime and C lobe is brown) is inactive and possibly autoinhibited by the N-terminal regulatory region (R, orange) containing two dsRBDs. (1) dsRNA (wavy lines) binding to the dsRBDs relieves autoinhibition and promotes catalytic-domain dimerization. (2) Catalytic-domain dimerization promotes autophosphorylation on activation-segment (purple) residue Thr446 (P). Three modes of autophosphorylation (depicted in blue) are possible. Phosphorylation of a PKR monomer in *cis* is unlikely because autophosphorylation displays second-order kinetics with respect to PKR concentration (Kostura and Mathews, 1989; Lemaire et al., 2005) and wt PKR phosphorylates a catalytically inactive kinase mutant (PKR-K296R) (Ortega et al., 1996; Thomis and Samuel, 1995), indicating that PKR autophosphorylation occurs in an intermolecular fashion. *Trans*-intradimer autophosphorylation is not likely, given the back-to-back orientation of the PKR dimer. *Trans*-interdimer autophosphorylation (i.e., dimers on dimers) is feasible and thus is the most likely mechanism of PKR autophosphorylation. (3) Autophosphorylation of PKR on Thr446 enhances PKR catalytic activity and is required for the specific recognition of eIF2α (green).

autophosphorylation, which in turn stabilizes dimerization.

We conclude that PKR activation-segment phosphorylation on Thr446 is critical for general activation of PKR catalytic efficiency, for stabilization of the PKR-KD dimer, and for eIF2α/K3L-specific substrate/pseudosubstrate recognition. A possible explanation for this complex interplay between dimerization, Thr446 activation-loop phosphorylation, catalytic activation, and specific eIF2α substrate recognition is provided by the crystal structure of the PKR•eIF2α complex (see Figure 7B in Dar et al., 2005). While dimerization and eIF2α binding occur on opposite ends of the protein kinase, the two are intimately linked by the central location of the activation segment. In addition, both the activation segment and the dimerization interface influence catalytic elements within the KD active site.

eIF2α Specificity Determinants Map to PKR Helix αG

Previous mutational studies mapped residues critical for PKR interaction to a conserved and common surface of eIF2α and K3L (Dar and Sicheri, 2002; Dey et al., 2005; Kawagishi-Kobayashi et al., 1997). In the PKR•eIF2α structure, this surface of eIF2α directly interacts with PKR helix αG (Figure 6A and Dar et al., 2005). Consistent with these structural observations, our analysis of the PKR-KD identified mutations at conserved residues Thr487 and Phe495 in helix αG that specifically impaired eIF2α, but not histone, phosphorylation. These results are consistent with the notion that histones only engage the phosphoacceptor binding site in PKR in the immediate vicinity of the active site, whereas eIF2α recognition involves bipartite interactions with both helix αG and the phosphoacceptor binding site. Thr487 is at the center of the eIF2α-specific binding site, which would account for the potent loss of eIF2α phosphorylation resulting from its mutation. In contrast, Phe495 does not contact eIF2α directly but instead lies at the interface between helix αG and the bulk of the kinase domain. Interestingly, helix αG adopts a novel position in PKR relative to other protein kinases, and this appears to contribute to eIF2α binding specificity (see Figure 4A in Dar et al., 2005). We posit that the PKR-F495P mutation may disrupt the integrity of helix αG or the position of helix αG relative to the kinase and hence would disrupt eIF2α binding indirectly.

Finally, mutations in helix αG of GCN2, like the PKR Thr487 mutations, specifically impaired eIF2α phosphorylation (Figures 5E and 5F). By extension, we propose that eIF2α recognition by PERK and HRI is likely also dependent on critical contacts with helix αG and the precise orientation of helix αG. The PKR-T487D mutant that is specifically defective for eIF2α phosphorylation but retains general kinase activity may be a useful tool to examine the role of PKR in cellular signaling pathways and identify alternate substrates. Comparing the phenotypes of *pkr*$^{-/-}$ and *PKR-T487D* knockin cells may help reveal roles for PKR that are independent of eIF2α phosphorylation. As all four eIF2α kinases dimer-

ize and autophosphorylate on a conserved Thr in the kinase activation segment, we propose that the PKR activation mechanism delineated in this manuscript linking kinase-domain dimerization and autophosphorylation with specific substrate recognition is likely conserved among all members of the eIF2α kinase family.

Experimental Procedures

Yeast Strains

Yeast strains H1894 (*MATa ura3-52 leu2-3 leu2-112 trp1-63 gcn2Δ*) (Kawagishi-Kobayashi et al., 1997), J80 (*MATa ura3-52 leu2-3 leu2-112 trp1-63 gcn2Δ sui2Δ* p[*SUI2*, *LEU2*]) and J82 (*MATa ura3-52 leu2-3 leu2-112 trp1-63 gcn2Δ sui2Δ* p[*SUI2-S51A*, *LEU2*]) (Ung et al., 2001), and H17 (*Matα gcn3-102 leu2-3 leu2-112 ura3-52*) (Harashima et al., 1987) were described previously. Chromosomal *SUI2* encoding yeast eIF2α in strain H2557 (*MATα ura3-52 leu2-3 leu2-112 gcn2Δ*) was replaced with *SUI2-S51A* to generate strain J223. Strain Y190 (*MATa leu2-3 leu2-112 ura3-52 trp1-Δ901 his3-200 ade2-101 gal4-Δ gal80-Δ URA3::GAL1-lacZ LYS2::GAL1-HIS3*) was used for two-hybrid analyses.

Plasmids, Mutagenesis, and Screens

See Supplemental Data.

Immunoblot Analysis of Protein Expression and Phosphorylation in Yeast

Transformants of strain H17 expressing PKR under control of the *GAL-CYC1* hybrid promoter were grown in SC-Ura (synthetic minimal medium with all amino acids, 2% glucose) medium overnight to saturation, diluted in fresh medium to OD_{600} ~ 0.1, and grown to OD_{600} ~ 0.6. Cells were harvested and transferred to SGal-Ura (SC-Ura except 10% galactose) medium for 2 hr to induce PKR expression. Transformants of H1894 expressing wt or mutant forms of GCN2 were grown in SC-Ura-His medium overnight to saturation, diluted in fresh medium to OD_{600} ~ 0.1, and grown to OD_{600} ~ 0.6. Then, 3-AT was added to 30 mM, and cells were harvested after 1 hr. Whole-cell extracts (WCEs) (4–5 μg) were resolved by SDS-PAGE and subjected to immunoblot analysis using antibodies specific for phospho-Ser51 on eIF2α (BioSource International or Cell Signaling), antibodies specific for phospho-Thr446 on PKR (Cell Signaling), polyclonal anti-yeast eIF2α antiserum, or monoclonal antibodies against an N-terminal epitope in human PKR (lot 71/10, RiboGene). To detect GCN2 expression, WCEs (25 μg) were resolved by SDS-PAGE and subjected to immunoblot analysis using polyclonal antiserum against the N terminus of GCN2 (Romano et al., 1998).

PKR and GCN2 In Vitro Kinase Assays

GST-eIF2α and His_6-eIF2$α_{1–200}$ were expressed in *E. coli* strain BL21(DE3) and purified using glutathione Sepharose 4B and Ni-silica resin, respectively, using the manufacturers' protocols. Flag- and His_6-tagged PKR derivatives were purified from yeast as described previously (Krishnamoorthy et al., 2001). Flag- and His_6-tagged GCN2 derivatives were partially purified by immunoprecipitation using anti-Flag M2 agarose as described previously (Dong et al., 2000). Phosphorylation of eIF2α by PKR or GCN2 was performed in kinase buffer (20 mM Tris-HCl [pH 8.0], 50 mM KCl, 25 mM $MgCl_2$, and 1 μM PMSF) with 10 μCi of [γ-^{33}P]ATP. Reactions were quenched after 20 min by addition of 2× SDS dye, products were separated by SDS-PAGE and stained with Coomassie blue, and the dried gel was subjected to autoradiography.

Recombinant histone 2A (H2A, Calbiochem) or 12-mer peptides Pept-S51 (ILLSELSRRRIR) and Pept-S51A (ILLSELARRRIR) were incubated with PKR and 10 μCi [γ-^{33}P]ATP in kinase buffer. Reactions were stopped after 20 min by addition of 2× SDS dye and products were separated by SDS-PAGE on 4%–20% Tris-glycine gels (H2A phosphorylation) or 10%–20% Tricin peptide gels (peptide phosphorylation). Gels were stained with Coomassie blue, dried, and then subjected to autoradiography. Incorporation of phosphate into H2A or peptides was determined using a phosphorimager. K_M calculations were performed using KaleidaGraph.

Analytical Ultracentrifugation

Equilibrium sedimentation was performed with a Beckman Optima XL-A ultracentrifuge and An60Ti rotor. PKR-KD ($PKR_{258–551}$-Δ13-H412N-C551A [Dar et al., 2005]) samples were prepared in 150 mM NaCl, 10 mM HEPES (pH 7.5), 3 mM DTT for analysis, and data for 30 μM, 15 μM, and 7.5 μM PKR solutions were collected at 4°C at speeds of 16,000, 19,000, and 22,000 rpm after 24 hr. Protein concentrations were determined by UV spectrometry at 280 nm using a molar extinction coefficient (ε = 27,310 $M^{-1}cm^{-1}$; A_{280nm} 0.1% = 0.836). Fitting to association models and K_d dimerization were determined using Origin software (Beckman).

Structural Models and Figures

Structural models were generated using the coordinates of the PKR•eIF2α complex (Dar et al., 2005) using PyMOL software (DeLano, 2004).

Supplemental Data

Supplemental Data include Supplemental Experimental Procedures, Supplemental References, and nine figures and can be found with this article online at http://www.cell.com/cgi/content/full/122/6/901/DC1/.

Acknowledgments

We thank members of the Dever, Sicheri, and Hinnebusch labs for advice and for discussions. This work was supported in part by the Intramural Research Program of the NIH, NICHD (T.E.D.) and by grants from the National Cancer Institute of Canada (F.S). A.C.D. is a recipient of a Canadian Graduate Scholarship from the Canadian Institutes for Health Research. F.S. is a recipient of a National Cancer Institute of Canada Scientist award.

Received: February 8, 2005
Revised: May 5, 2005
Accepted: June 29, 2005
Published: September 22, 2005

References

Carpick, B.W., Graziano, V., Schneider, D., Maitra, R.K., Lee, X., and Williams, B.R.G. (1997). Characterization of the solution complex between the interferon-induced, double-stranded RNA-activated protein kinase and HIV-I trans-activating region RNA. J. Biol. Chem. *272*, 9510–9516.

Chong, K.L., Feng, L., Schappert, K., Meurs, E., Donahue, T.F., Friesen, J.D., Hovanessian, A.G., and Williams, B.R.G. (1992). Human p68 kinase exhibits growth suppression in yeast and homology to the translational regulator GCN2. EMBO J. *11*, 1553–1562.

Cosentino, G.P., Venkatesan, S., Serluca, F.C., Green, S.R., Mathews, M.B., and Sonenberg, N. (1995). Double-stranded-RNA-dependent protein kinase and TAR RNA-binding protein form homo- and heterodimers *in vivo*. Proc. Natl. Acad. Sci. USA *92*, 9445–9449.

Dar, A.C., and Sicheri, F. (2002). X-ray crystal structure and functional analysis of vaccinia virus K3L reveals molecular determinants for PKR subversion and substrate recognition. Mol. Cell *10*, 295–305.

Dar, A.C., Dever, T.E., and Sicheri, F. (2005). Higher-order substrate recognition of eIF2α by the RNA-dependent protein kinase PKR. Cell *122*, this issue, 887–900.

DeLano, W.L. (2004). The PyMOL User's Manual (San Carlos, CA: Delano Scientific).

Delepine, M., Nicolino, M., Barrett, T., Golamaully, M., Lathrop, G.M., and Julier, C. (2000). *EIF2AK3*, encoding translation initiation factor 2-α kinase *3*, is mutated in patients with Wolcott-Rallison syndrome. Nat. Genet. *25*, 406–409.

Dever, T.E. (2002). Gene-specific regulation by general translation factors. Cell *108*, 545–556.

Dever, T.E., Chen, J.J., Barber, G.N., Cigan, A.M., Feng, L., Donahue, T.F., London, I.M., Katze, M.G., and Hinnebusch, A.G. (1993). Mammalian eukaryotic initiation factor 2α kinases functionally sub-

stitute for GCN2 in the *GCN4* translational control mechanism of yeast. Proc. Natl. Acad. Sci. USA *90*, 4616–4620.

Dey, M., Trieselmann, B.A., Locke, E.G., Lu, J., Cao, C., Dar, A.C., Krishnamoorthy, T., Dong, J., Sicheri, F., and Dever, T.E. (2005). PKR and GCN2 kinases and guanine nucleotide exchange factor eukaryotic translation initiation factor 2B (eIF2B) recognize overlapping surfaces on eIF2α. Mol. Cell. Biol. *25*, 3063–3075.

Dhaliwal, S., and Hoffman, D.W. (2003). The crystal structure of the N-terminal region of the alpha subunit of translation initiation factor 2 (eIF2α) from Saccharomyces cerevisiae provides a view of the loop containing serine *51*, the target of the eIF2α-specific kinases. J. Mol. Biol. *334*, 187–195.

Dong, J., Qiu, H., Garcia-Barrio, M., Anderson, J., and Hinnebusch, A.G. (2000). Uncharged tRNA activates GCN2 by displacing the protein kinase moiety from a bipartite tRNA-binding domain. Mol. Cell *6*, 269–279.

Harashima, S., Hannig, E.M., and Hinnebusch, A.G. (1987). Interactions between positive and negative regulators of *GCN4* controlling gene expression and entry into the yeast cell cycle. Genetics *117*, 409–419.

Hinnebusch, A.G. (2000). Mechanism and regulation of initiator methionyl-tRNA binding to ribosomes. In Translational Control of Gene Expression, N. Sonenberg, J.W.B. Hershey, and M.B. Mathews, eds. (Cold Spring Harbor, NY: Cold Spring Harbor Laboratory Press), pp. 185–243.

Kawagishi-Kobayashi, M., Silverman, J.B., Ung, T.K., and Dever, T.E. (1997). Regulation of the protein kinase PKR by the vaccinia virus pseudosubstrate inhibitor K3L is dependent on residues conserved between the K3L protein and the PKR substrate eIF2α. Mol. Cell. Biol. *17*, 4146–4158.

Kostura, M., and Mathews, M.B. (1989). Purification and activation of the double-stranded RNA-dependent eIF-2 kinase DAI. Mol. Cell. Biol. *9*, 1576–1586.

Krishnamoorthy, T., Pavitt, G.D., Zhang, F., Dever, T.E., and Hinnebusch, A.G. (2001). Tight binding of the phosphorylated α subunit of initiation factor 2 (eIF2α) to the regulatory subunits of guanine nucleotide exchange factor eIF2B is required for inhibition of translation initiation. Mol. Cell. Biol. *21*, 5018–5030.

Langland, J.O., and Jacobs, B.L. (1992). Cytosolic double-stranded RNA-dependent protein kinase is likely a dimer of partially phosphorylated M_r = 66,000 subunits. J. Biol. Chem. *267*, 10729–10736.

Lemaire, P.A., Lary, J., and Cole, J.L. (2005). Mechanism of PKR activation: dimerization and kinase activation in the absence of double-stranded RNA. J. Mol. Biol. *345*, 81–90.

Mellor, H., and Proud, C.G. (1991). A synthetic peptide substrate for initiation factor-2 kinases. Biochem. Biophys. Res. Commun. *178*, 430–437.

Nanduri, S., Rahman, F., Williams, B.R., and Qin, J. (2000). A dynamically tuned double-stranded RNA binding mechanism for the activation of antiviral kinase PKR. EMBO J. *19*, 5567–5574.

Nonato, M.C., Widom, J., and Clardy, J. (2002). Crystal structure of the N-terminal segment of human eukaryotic translation initiation factor 2α. J. Biol. Chem. *277*, 17057–17061.

Ortega, L.G., McCotter, M.D., Henry, G.L., McCormack, S.J., Thomis, D.C., and Samuel, C.E. (1996). Mechanism of interferon action. Biochemical and genetic evidence for the intermolecular association of the RNA-dependent protein kinase PkR from human cells. Virology *215*, 31–39.

Romano, P.R., Green, S.R., Barber, G.N., Mathews, M.B., and Hinnebusch, A.G. (1995). Structural requirements for double-stranded RNA binding, dimerization, and activation of the human eIF-2α kinase DAI in *Saccharomyces cerevisiae*. Mol. Cell. Biol. *15*, 365–378.

Romano, P.R., Garcia-Barrio, M.T., Zhang, X., Wang, Q., Taylor, D.R., Zhang, F., Herring, C., Mathews, M.B., Qin, J., and Hinnebusch, A.G. (1998). Autophosphorylation in the activation loop is required for full kinase activity in vivo of human and yeast eukaryotic initiation factor 2α kinases PKR and GCN2. Mol. Cell. Biol. *18*, 2282–2297.

Tan, S.L., Gale, M.J., and Katze, M.G. (1998). Double stranded RNA-independent dimerization of the interferon-induced protein kinase PKR and inhibition of dimerization by the cellular P58 IPK inhibitor. Mol. Cell. Biol. *18*, 2431–2443.

Thomis, D.C., and Samuel, C.E. (1995). Mechanism of interferon action: characterization of the intermolecular autophosphorylation of PKR, the interferon-inducible, RNA-dependent protein kinase. J. Virol. *69*, 5195–5198.

Ung, T.L., Cao, C., Lu, J., Ozato, K., and Dever, T.E. (2001). Heterologous dimerization domains functionally substitute for the double-stranded RNA binding domains of the kinase PKR. EMBO J. *20*, 3728–3737.

Wu, S., and Kaufman, R.J. (1997). A model for the double-stranded RNA (dsRNA)-dependent dimerization and activation of the dsRNA-activated protein kinase PKR. J. Biol. Chem. *272*, 1291–1296.

Zhang, F., Romano, P., Nagamura-Inoue, T., Tian, B., Dever, T.E., Mathews, M.B., Ozato, K., and Hinnebusch, A.G. (2001). Binding of double-stranded RNA to protein kinase PKR is required for dimerization and promotes critical autophosphorylation events in the activation loop. J. Biol. Chem. *276*, 24946–24958.